Motion of Particles Adhering to the Leading Lamella of Crawling Cells

MICAH DEMBO and ALBERT K. HARRIS
Theoretical Division, Los Alamos National Laboratory, Los Alamos, New Mexico 87545, and Department of Zoology, University of North Carolina, Chapel Hill, North Carolina 27514

ABSTRACT Time-lapse films of particle motion on the leading lamella of chick heart fibroblasts and mouse peritoneal macrophages were analyzed. The particles were composed of powdered glass or powdered aminated polystyrene and were 0.5–1.0 μm in radius. Particle motions were described by steps in position from one frame of the time-lapse movies to the next. The statistics of the step-size distribution of the particles were consistent with a particle in Brownian motion subject to a constant force. From the Brownian movement, we have calculated the two-dimensional diffusion coefficient of different particles. These vary by more than an order of magnitude (10^{-11}–10^{-10} cm^2/s) even for particles composed of the same material and located very close to each other on the surface of the cell. This variation was not correlated with particle size but is interpretable as a result of different numbers of adhesive bonds holding the particles to the cells. The constant component of particle movement can be interpreted as a result of a constant force acting on each particle ($0.1–1.0 \times 10^{-8}$ dyn). Variations in the fractional coefficient for particles close to each other on the cell surface do not yield corresponding differences in velocity, suggesting that the frictional coefficient and the driving force vary together. This is consistent with the hypothesis that the particles are carried by flow of the membrane as a whole or by flow of some submembrane material. The utility of our methods for monitoring cell motile behavior in biologically interesting situations, such as a chemotactic gradient, is discussed.

It has been shown by a number of authors (1, 12, 15) that, when the leading edge of a moving cell contacts a small particle, the particle is frequently "picked up" by the cell and transported backward over or under the leading lamella. If transported on the upper surface of the lamella, the particles usually come to rest at the margin of the lamelloplasm and the granular endoplasm. Many different cell types (e.g., fibroblasts [5], epithelial cells [9], and nerve cells [4]) have been shown to transport particles in this manner. Furthermore, particles composed of many different materials (e.g., polystrene, glass, charcoal, gold, and cancanavalin A–treated erythrocytes) can be transported.

Detailed photographic records of the tracks of particles as they are transported over the leading lamella have been reported by several authors (1, 11, 12). In addition to the general transport of the particles from the front toward the back of the cells, these records reveal that the individual positional changes undergone by the particles during fixed time intervals are highly variable. This result indicates the existence of both constant and random components to the forces causing particle motion.

When the leading lamella contacts a particle, it has no way to tell whether or not the particle is fixed to the surface over which the cell is moving. Consequently, the forces that pull particles backward over the leading lamella are presumably related to the forces by which the leading lamella pulls the cell forward. Time-lapse films of particle motion thus offer a potential means of obtaining quantitative information on the mechanism of cell propulsion.

MATERIALS AND METHODS

Filming

Time-lapse films of cells transporting particles were obtained by one of us (A. K. Harris). The methodology used to prepare the cells for filming particle transport has been described previously (12). The time interval between successive exposures of the film was fixed at 10 s. Two typical film sequences, each of a single cell, were selected for analysis on the basis of clarity of resolution. One of the film sequences was of a chick heart fibroblast (CHF) cell transporting particles

THE JOURNAL OF CELL BIOLOGY · VOLUME 91 NOVEMBER 1981 528-536

of aminated polystyrene (cation exchange resin). The second film sequence was of a mouse peritoneal macrophage (MPM) transporting particles of powdered glass.

Selection of Particles for Analysis

Groups of particles observed in a sequence of film were called "cohorts." The film of a cohort of particles was considered satisfactory for detailed analysis if it satisfied the following criteria:

(*a*) The largest distance between two members of the cohort was <15 μm at the start of the period of observation.

(*b*) All members of a cohort should be clearly visible in all successive frames during the period of observation.

(*c*) All members of a cohort were >2 μm behind the leading edge of the cell at the start of the period of observation.

(*d*) All members of a cohort were >2 μm in front of the edge of the granular cytoplasm at the end of the period of observation.

(*e*) All members of a cohort were free from collisions with other particles or debris during the period of observation.

(*f*) All members of the cohort were on the upper surface of the leading lamella.

It has been found (8, 12) that particles of various materials moved significantly faster during the 1st min after being picked up by the cell than during subseqeunt 1-min time intervals. Our decision to concentrate only on particles that had moved away from the leading edge (criterion *c*) was made in an effort to avoid any transient effects associated with the initial attachment of particles or the motion of the leading edge.

Many particles were transported by the CHF cell, and two cohorts that satisfied the criteria for at least three minutes were selected at random. One of the cohorts had three members and the other had four members.

Only three particles were transported by the MPM. Two of the particles were in the same cohort and the third was isolated. Individual particles will be designated by referring to an index, k, between 1 and 10. The cohort to which a particle belongs as well as other physical information can be determined from its index by referring to Table I.

Recording the Raw Data

Films were projected onto graph paper using a photo-optical data analyzer, model 224A, manufactured by L. W. International, Woodland Hills, Calif. The X and Y coordinates of the centers of the particles in a cohort were recorded on each frame. The accuracy of these measurements is discussed in the final part of Materials and Methods. To determine objectively the motion of the cell as a whole, we also recorded the positions of four cytoplasmic granules in the granular cytoplasm behind the leading lamella. The granules moved in a correlated fashion even over 10-s time intervals, and the center of mass of the four granules therefore gave a good index of overall cell displacement.

First-stage Data Reduction

The raw data for a cohort with ℓ members consisted of a sequence of values $(\tilde{X}_{0,k}\tilde{Y}_{0,k}), (\tilde{X}_{1,k}\tilde{Y}_{1,k}) \ldots (\tilde{X}_{n,k}\tilde{Y}_{n,k})$ for the X and Y coordinates in successive frames for each particle $k = k_1, k_2 \ldots k_\ell$. There was also a sequence of coordinate values $(\tilde{X}_{0,m}\tilde{Y}_{0,m}), (\tilde{X}_{1,m}\tilde{Y}_{1,m}) \ldots (\tilde{X}_{n,m}\tilde{Y}_{n,m})$ for the center of mass, m, of the four cytoplasmic granules. We first corrected the particle motion for the motion of the cell as a whole by numerically translating the coordinate system so that it was fixed with respect to the center of mass. This yielded values $(\hat{X}_{i,k}\hat{Y}_{i,k})$ for the position of a particles in the new coordinates where

$$\hat{X}_{i,k} = \tilde{X}_{i,k} - \tilde{X}_{i,m} + \tilde{X}_{0,m} \tag{1a}$$

and

$$\hat{Y}_{i,k} = \tilde{Y}_{i,k} - \tilde{Y}_{i,m} + \tilde{Y}_{0,m} \tag{1b}$$

for $i = 0, 1, 2 \ldots n$, $k = k_1, k_2 \ldots k_\ell$.

To have some basis for comparing coordinate systems from one cohort to another, we rotated the coordinate system for each cohort so that the angular orientation of the X-axis was parallel to the average direction of motion of the particles. For example, the average displacements in the X and Y directions for a cohort with ℓ members are

$$\overline{\Delta X} = \frac{1}{\ell}\sum_{k=1}^{\ell}(\hat{X}_{0,k} - \hat{X}_{n,k}) \tag{2a}$$

and

$$\overline{\Delta Y} = \frac{1}{\ell}\sum_{k=1}^{\ell}(\hat{Y}_{0,k} - \hat{Y}_{n,k}). \tag{2b}$$

We would therefore rotate the coordinate system through an angle

$$\phi = \arctan(\overline{\Delta Y}/\overline{\Delta X}). \tag{2c}$$

The sequence of coordinates for a particle in this final coordinate system $(X_{i,k}Y_{i,k})$ is given by

$$X_{i,k} = \hat{X}_{i,k}\cos(\phi) + \hat{Y}_{i,k}\sin(\phi) \tag{3a}$$

and

$$Y_{i,k} = -\hat{X}_{i,k}\sin(\phi) + \hat{Y}_{i,k}\cos(\phi) \tag{3b}$$

for $i = 0, 1, 2 \ldots n$, $k = k_1, k_2 \ldots k_\ell$. Subsequent analysis of the data will be described as each aspect is dealt with in Results.

TABLE I

Index of Particles

Index k	Cohort number	Cell type*	Particle type‡	Cross-sectional area of particle	Time of observation
				$\times 10^{-8}$ cm^2	s
1	1	CHF	AP	0.9	180
2	1	CHF	AP	0.9	180
3	1	CHF	AP	0.6	180
4	1	CHF	AP	1.5	180
5	2	CHF	AP	1.0	240
6	2	CHF	AP	0.9	240
7	2	CHF	AP	1.2	240
8	3	MPM	PG	2.0	850
9	3	MPM	PG	2.0	850
10	4	MPM	PG	2.8	500

* *CHF*, chick heart fibroblast; *MPH*, mouse peritoneal macrophage.
‡ *AP*, aminated polystyrene; *PG*, powdered glass.

Errors in Position Measurements

In a given photographic image of a particle, the uncertainty in locating the $\tilde{X}$ or $\tilde{Y}$ coordinates of the center had a σ value of ≈5% of the mean particle radius. An independent source of experimental error arose because of changes in the actual image of a particle resulting from variations of the intersection of the particle with the plain of focus of the microscope. It is difficult to determine the exact magnitude of the σ value for this source of error, but we feel that a conservative upper limit is ≈10% of the mean particle radius. Because the center of mass of the cell was determined from the mean of four measurements, the variance of each coordinate was one quarter the variance for a single measurement.

If we take 0.75 μm as a typical value of the mean particle radius (see Table I), then the variance of the X and Y coordinates of a particle attributable to experimental error is $\sigma_{er}^2 \leq [(0.05 \times 0.75)^2 + (0.10 \times 0.75)^2][1 + 0.25] = 0.009$ μm^2. Finally, it must be remembered that changes in particle position are determined from the difference between two measured coordinate values. Consequently, the variance in changes of position attributable to experimental error will be ≤0.02 μm^2.

RESULTS

Fig. 1 shows a tracing of the initial and final positions of the particles in one of the cohorts studied. This figure also shows the initial and final positions of cytoplasmic granules used to index cell motion as well as the corresponding outlines of the front and back edges of the leading lamella. Notice that gross motion of the particles is from the front toward the back of the cell, opposite to the general direction of cell motion. When viewed on this long time scale, all the particles in a cohort move more or less in the same direction and the magnitude of the displacement of the particles in a cohort is also approximately equal.

In the case of the aminated polystyrene particles moving on the CHF cell it was only possible to observe a cohort for between 180 and 240 s. This was mainly because of the high velocity of particle transport. The powdered glass particles on the MPM cell could be observed for between 500 and 850 s. This meant that the sampling error in determining the properties of particle motion on the CHF cell was considerably greater than the sampling error on the MPM cell. To compensate for this factor, we analyzed a larger number of particles on the CHF cell.

Fig. 2 shows a more detailed view of the tracks of the particles in the cohort shown in Fig. 1. These data have been corrected for the motion of the cell as a whole, as described in Materials and Methods. We have also rotated the coordinate system so that the particles in the cohort move in the direction of the positive X axis.

The particle tracks in Fig. 2 illustrate the marked random component of the particle motion. It is evident that the details of the direction and magnitude of the positional changes undergone by the three particles are highly variable.

The uppermost particle track in Fig. 2 gives the qualitative impression of a greater degree of "randomness" or variability in the individual positional charges. The other cohorts observed also give the impression of considerable differences from particle to particle in the degree of randomness. We will subsequently show that these differences are statistically significant.

The change in position of a particle during the ith time interval is given by the vector

$$(\Delta X_{i,k}\ \Delta Y_{i,k}) = ([X_{i,k} - X_{i-1,k}][Y_{i,k} - Y_{i-1,k}]) \qquad (4)$$

for $i = 1, 2 \ldots n$.

Fig. 3 *a* and *b* shows histograms of the probability of different values of $\Delta X_{i,k}$ and $\Delta Y_{i,k}$ for particle 9, i.e., a powdered glass particle. The solid curves in Fig. 3 *a* and *b* shows the maximum likelihood fit of the probability distributions to a Gaussian. Similar satisfactory fits were obtained for the step-size distributions in both the X and Y directions for all the particles studied. A typical example of the fits obtained for the aminated polystyrene particles is shown in Fig. 3 *c* and *d*. The scatter of the data was always within the expected sampling error.

Fitting of the step-size distributions to the Gaussian yielded nonbiased estimates of the mean step size that a particle takes in the X and Y directions

$$\hat{\mu}_{x,k} = \frac{1}{n}\sum_{i=1}^{n} \Delta X_{i,k} \qquad (5a)$$

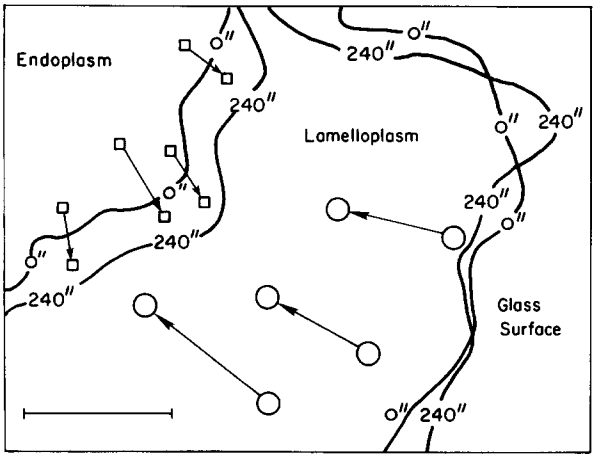

FIGURE 1 Initial and final positions of the particles in cohort 2 (circles). From left to right the particles are numbers 5, 6, and 7. Also shown are the initial and final positions of four cytoplasmic granules (squares). The lines in the upper left indicate the initial and final positions of the margin between the endoplasm and the leading lamella. The two lines to the right indicate the initial and final positions of the leading edge of the cell. The time change between initial and final positions was 240 s. Bar, 10 μm.

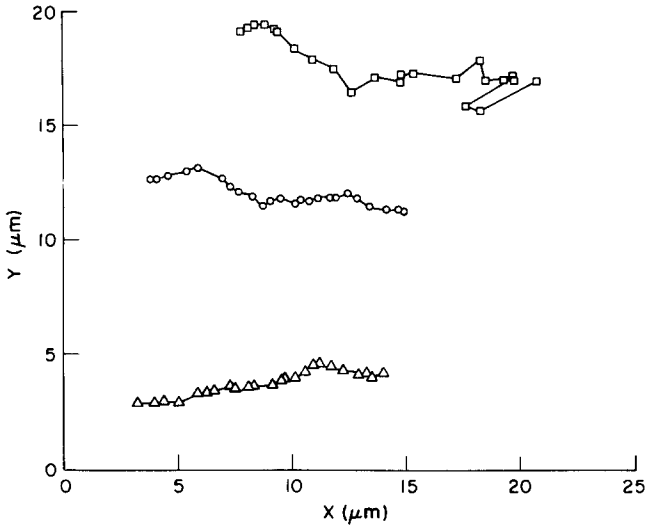

FIGURE 2 A detailed view of the paths of the three particles in cohort 2. From top to bottom the particles are numbers 5, 6, and 7. These data have been corrected for the motion of the cell as described in Materials and Methods. In addition, the coordinates have been rotated so that the particles move in the direction of the positive X-axis. Symbols represent the position of the particles at 10-s intervals.

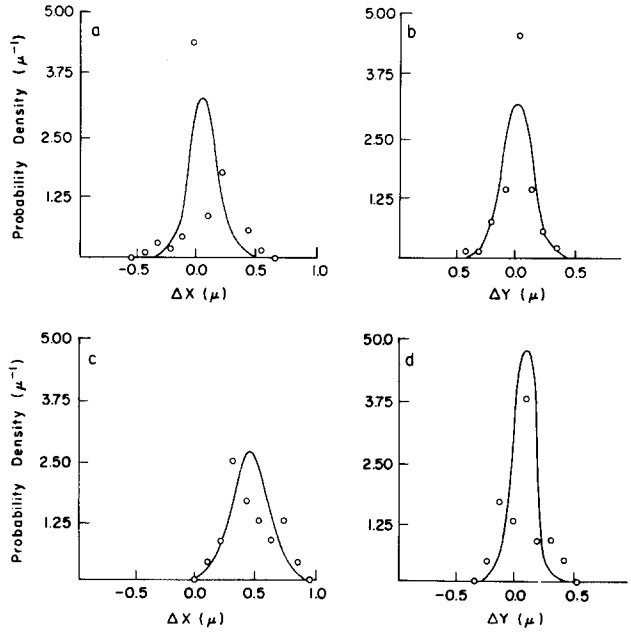

FIGURE 3 Step-size distributions of two particles in the X and Y directions. (*a*) Distribution of ΔX for particle 9; (*b*) distribution of ΔY for particle 9; (*c*) distribution of ΔX for particle 7; (*d*) distribution of ΔY for particle 7. The data points represent the observed probability density of step sizes in a small interval. The solid curve shows the maximum likelihood fit of these data to a Gaussian.

and

$$\hat{\mu}_{y,k} = \frac{1}{n}\sum_{i=1}^{n} \Delta Y_{i,k}, \tag{5b}$$

where k denotes the particle index. We also obtain unbiased estimates of the variations of the step-size distributions

$$\hat{\sigma}^2_{x,k} = \frac{1}{n-1}\sum_{i=1}^{n} (\Delta X_{i,k} - \hat{\mu}_{X,k})^2 \tag{6a}$$

and

$$\hat{\sigma}^2_{y,k} = \frac{1}{n-1}\sum_{i=1}^{n} (\Delta Y_{i,k} - \hat{\mu}_{Y,k})^2. \tag{6b}$$

The sample means and variances can be used to obtain confidence limits for the population means and variances by standard statistical techniques. Table II gives a summary of the 95% confidence limits of the various populations parameters for all the particles studied. These data are presented in the form: midpoint of confidence interval ± one-half width of confidence interval. The midpoint of the confidence interval does not correspond to the most probable value of the population parameter except in the case of the means. In the case of the variances the midpoint is between 6 and 30% larger than the most probable value depending on the sample size.

Application of the F test to the data of Table II shows that there is no detectable difference between the values of $\hat{\mu}_x$ for particles within the same cohort. In addition, none of the values of $\hat{\mu}_y$ are detectably different from zero. This is simply quantitative proof of the previous qualitative observation that particles in the same cohort seem to move at the same average speed and in the same average direction.

This result is in accord with the observations of DiPasquale (8). He observed no detectable differences in the average velocities of ruffles, blebs, latex beads, and concanavalin A–coated erythrocytes on various kinds of epithelial cells. It thus seems clear that the average speed of transport on the leading lamella is a property of the lamella and does not depend on the thing that is transported.

Fig. 4 shows a scattergram of the correlation between the maximum likelihood estimates of $\sigma_{y,k}$ and $\sigma_{x,k}$ for different particles. As can be seen, these data are highly correlated. Furthermore, the scatter of the data on either side of the line $\sigma_{y,k} = \sigma_{x,k}$ is within the limits of reasonable sampling error. We therefore cannot reject the important hypothesis that $\sigma^2_{y,k} = \sigma^2_{x,k}$ for all particles. This is quite remarkable when we consider that the coordinate system was chosen so that the average direction of motion of the particles was always parallel to the X direction. We thus conclude that there is no detectable tendency for the variation in step size to be larger in the average direction of motion than in the direction perpendicular to the average direction of motion.

In interpreting these observations, we considered two general types of hypothesis about the nature of the forces on the particles. One hypothesis was that the cell exerts a constant force on the particles and that the apparent randomness in particle motion is attributable to thermal agitation. The second hypothesis was that the force exerted by the cell has some directionality but that it is also highly variable with time and thus produces both the constant and random components of the particle motion by one mechanism. Our observation that the variable component of particle motion does not have the same spatial directionality as the constant component argues against the second hypothesis. This does not mean that there is no variable component to the force that the cell exerts on a particle, but it does suggest that this source of variable force is small compared to externally generated variable forces on the particles.

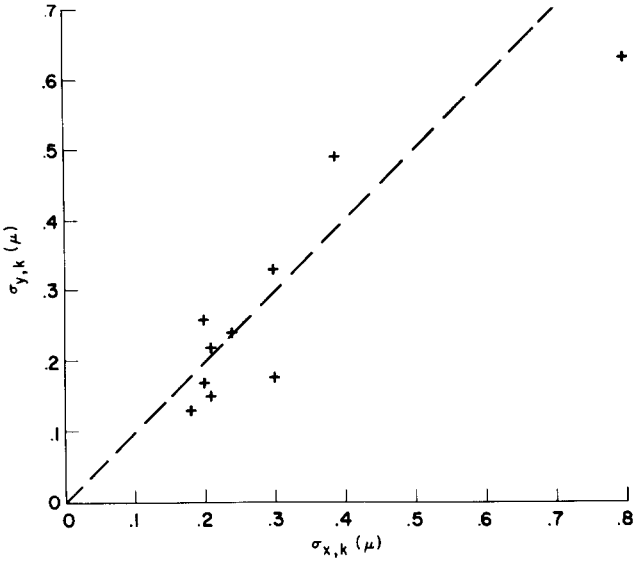

FIGURE 4 Scattergram showing the correlation between $\sigma_{y,k}$ and $\sigma_{x,k}$ for the 10 particles studied. The dashed line indicates the expected regression curve if $\sigma_{y,k} = \sigma_{x,k}$; the data do not depart significantly from this curve.

TABLE II

95% Confidence Limits for Parameters of Step-size Distributions*

Index k	$\mu_{x,k}$‡	$\mu_{y,k}$‡	$\sigma^2_{x,k}$§	$\sigma^2_{y,k}$§	$\sigma^2_{p,k}$§
1	+0.19 ± 0.20	−0.08 ± 0.25	+0.213 ± 0.125	+0.334 ± 0.201	+0.232 ± 0.104
2	+0.32 ± 0.10	+0.05 ± 0.07	+0.064 ± 0.037	+0.031 ± 0.019	+0.039 ± 0.018
3	+0.30 ± 0.15	+0.05 ± 0.±0	+0.125 ± 0.075	+0.048 ± 0.029	+0.073 ± 0.032
4	+0.29 ± 0.10	−0.03 ± 0.13	+0.057 ± 0.034	+0.098 ± 0.059	+0.067 ± 0.030
5	+0.57 ± 0.35	+0.06 ± 0.28	+0.819 ± 0.441	+0.514 ± 0.277	+0.592 ± 0.232
6	+0.49 ± 0.10	+0.03 ± 0.10	+0.058 ± 0.031	+0.064 ± 0.035	+0.054 ± 0.021
7	+0.46 ± 0.08	−0.08 ± 0.08	+0.050 ± 0.027	+0.035 ± 0.019	+0.038 ± 0.015
8	+0.08 ± 0.06	+0.00 ± 0.04	+0.100 ± 0.029	+0.114 ± 0.033	+0.102 ± 0.022
9	+0.08 ± 0.04	+0.00 ± 0.03	+0.036 ± 0.011	+0.018 ± 0.005	+0.026 ± 0.006
10	+0.12 ± 0.07	+0.00 ± 0.07	+0.063 ± 0.023	+0.066 ± 0.024	+0.061 ± 0.017

* The step size is defined as the positional change in the 10-s time interval.
‡ × 10^4 cm.
§ × 10^8 cm^2.

On the assumption that this conclusion is correct, we can refine our estimates of the variation of the step size distribution by pooling the information from both the X and Y coordinates into a single estimate

$$\hat{\sigma}^2_{p,k} = \frac{1}{2}[\hat{\sigma}^2_{x,k} + \hat{\sigma}^2_{y,k}] \tag{7}$$

This will yield tighter confidence intervals on the pooled population variance, $\sigma^2_{p,k}$, since the number of degrees of freedom is increased by a factor of two. Refined confidence intervals obtained by this procedure are given in the last column of Table II.

In Materials and Methods, we estimated an upper limit of 0.02 μm^2 for the apparent variation in step size resulting from experimental error, σ^2_{er}. From Table II we see that the values of $\sigma^2_{p,k}$ for all but one of the particles are much larger than this upper bound. This indicates that, although experimental error may contribute to the value of $\sigma^2_{p,k}$, experimental error cannot explain all, or even most, of the observed variation. Consequently there is a truly stochastic component to the motion of the particles we have studied.

If the values of $\sigma^2_{p,k}$ for different particles are compared, it is immediately apparent that very significant differences occur. This is true even for particles that are within the same cohort and therefore have approximately the same average step size. It is difficult to see how the variable component of motion could change by a factor of 10 for two particles that are within a few microns of each other and that have the same constant component of motion. Consequently, this observation should be explained by any complete model of particle motion.

To further explore the statistical properties of the motion of the particles, we carried out a number of tests for correlation or independence of various matched pairs of observations.

Three statistical measures of correlation were used: the classical correlation coefficient, ρ, which is efficient if the two variables have Gaussian distributions; and two robust nonparametric statistics, Kendall's rank correlation coefficient, τ_k, and Spearman's rank correlation coefficient, r_s. These last two statistics are nearly as efficient as the correlation coefficient for Gaussian variables and do not break down in most non-Gaussian situations. In general, all three of these measures gave the same results for Gaussian variables; for non-Gaussian variables, ρ gave erratic results, whereas τ_k and r_s agreed. In light of this, we will simply present the results obtained with τ_k.

For a set of n ordered pairs of observations

$$\begin{matrix} a_i \\ b_i \end{matrix} \; i = 1, 2 \ldots n,$$

τ_k is defined as

$$\tau_k \equiv \frac{2}{n(n-1)} \sum_{i=1}^{n-1} \sum_{j=i+1}^{n} \text{sign}[(a_i - a_j)(b_i - b_j)], \tag{8a}$$

where for an arbitrary number z

$$\text{sign}(z) \equiv \begin{matrix} +1 \text{ if } z > 0 \\ 0 \text{ if } z = 0 \\ -1 \text{ if } z < 0. \end{matrix} \tag{8b}$$

Note that according to this definition τ_k is +1 if there is a perfect positive correlation between the b_i and the a_i and is equal to −1 if there is a perfect negative correlation. If the absolute value of τ_k exceeds a certain 0.05 critical value, then we can reject the hypothesis that the a_i and b_i are independent with 95% confidence. The critical value depends on the sample size, but standard tables are available (6).

If a particle takes a bigger (or smaller) than average step in the X (or Y) direction, does it tend to take another big or small step during the next time interval? This possibility can be tested by calculating τ_k for succeeding step sizes in the X and Y directions. The first two columns of Table III show the results of this calculation. As can be seen, no hint of correlation was found for any of the particles. This effectively eliminates the possibility that there are extended sequences where a particle moves rapidly interspersed with other sequences where it moves slowly. It also eliminates the possibility that there are any significant changes in the overall direction of particle motion during the period of observation.

It is well known that the mean and variance of the sum of n independent random variables drawn from the same population is proportional to n. Consequently, the results in lines *1* and *2* of Table III imply that the values of μ_x, σ^2_x, and σ^2_y will change linearly with the period between observations Δt. We have confirmed this conclusion by direct observation for time intervals of up to 30 s (data not shown).

The independence of the step sizes during subsequent time intervals is a useful check on the conclusion that the variation in step size results from true stochastic behavior and not from experimental error. This is because variation resulting from experimental error does not depend on the time interval between observations, whereas the observed variation grows linearly with time interval.

If a particle takes an unusually small (or large) step in the X direction, does it tend to take a simultaneous small (or large) step in the Y direction? This possibility can be checked by looking for correlations between

$$V(\Delta X_{i,k}) \equiv (\Delta X_{i,k} - \mu_{x,k})^2 \tag{9a}$$

and

$$V(\Delta X_{i,k}) \equiv (\Delta Y_{i,k} - \mu_{y,k})^2 \tag{9b}$$

The line *3* in Table III shows the values of τ_k for correlation between $V(\Delta X_{i,k})$ and $V(\Delta Y_{i,k})$. As shown, no significant correlations were found except for the two particles of cohort 3, i.e., particles 8 and 9. Furthermore, although the correlations found for particles 8 and 9 are highly significant from a

TABLE III

Kendall's Statistic for Correlation between Paired Observations* $\begin{matrix} a_i \\ b_i \end{matrix}$

Index k	$\Delta X_{i,k}$ / $\Delta X_{i+1,k}$	$\Delta Y_{i,k}$ / $\Delta Y_{i+1,k}$	$V(\Delta X_{i,k})$‡ / $V(\Delta Y_{i,k})$	$V(\Delta X_{i,k})$‡ / $V(\Delta Y_{i+1,k})$	$V(\Delta X_{i,k})$‡§ / $V(\Delta Y_{i,k})$	0.95 Critical Value
1	+0.05	−0.32	+0.24	+0.02	+0.27	±0.35
2	−0.10	+0.10	+0.22	−0.27	+0.22	±0.35
3	+0.08	−0.10	+0.10	+0.08	+0.10	±0.35
4	+0.02	−0.12	+0.01	+0.15	+0.01	±0.35
5	+0.24	−0.10	+0.26	+0.19	+0.26	±0.30
6	−0.03	+0.06	−0.16	+0.00	−0.16	±0.30
7	−0.11	−0.05	−0.04	−0.21	−0.04	±0.30
8	+0.02	−0.12	+0.27	−0.08	+0.06	±0.15
9	−0.08	+0.00	+0.29	−0.01	−0.04	±0.15
10	−0.14	−0.16	−0.02	−0.07	−0.02	±0.20

* τ_k, defined by Eq. 8 *a*.
‡ See Eq. 9 *a* and *b* for definition of $V(\Delta X_{i,k})$ and $V(\Delta X_{i,k})$.
§ Restricted to these i for which $|\Delta X_{i,k}| + |\Delta Y_{i,k}| > 0.05$ μm.

statistical viewpoint (less than one chance in 1,000), they are very small in the physical sense.

A hint as to what was causing the correlations in particles 8 and 9 was obtained from the histograms of the step-size distribution for these particles. As illustrated by particle 9 in Fig. 3 *a* and *b*, both these particles showed an unusually high incidence of steps in which no motion took place.

The significant values of the τ_k statistic in line *3* of Table III apparently arise because the periods of immobilization in the *X* direction are associated with the periods of immobilization in the *Y* direction. This conclusion is supported by the absence of correlations between $V(\Delta X_{i,k})$ and $V(\Delta Y_{i+1,k})$ (line *4* of Table III), and the absence of correlation between $V(\Delta X_{i,k})$ and $V(\Delta Y_{i,k})$ if steps where $|\Delta X_{i,k}| + |\Delta Y_{i,k}|$ is <0.05 μm are eliminated from consideration (line *5* of Table III). This conclusion was also checked by dividing the random walks for particles 8 and 9 into two halves and repeating statistical tests on each half separately. All of the statistical features of the walks (including the τ_k values) were the same for the first and second halves.

We thus conclude that the small departure from statistical independence indicated by the τ_k values in line *3* are attributable to a small number of randomly scattered incidents of temporary immobilization during which the particles just seemed to stop all motion as though striking an invisible obstacle.

An additional class of questions involving the technique of finding correlations between paired observations concerns the relationship between the sizes of the steps taken by two different particles in a cohort, during the same time interval. Table IV shows an analysis entirely similar to that carried out in Table III. This analysis revealed no correlation between $\Delta Y_{i,k}$ and $\Delta Y_{i,j}$ for any of the 10 possible pairs of particles, both taken from the same cohort, except for particles 8 and 9. A similar result was obtained for correlation between $\Delta X_{i,k}$ and $\Delta X_{i,j}$ (data not shown).

The correlation found between particles 8 and 9 is significant but is even weaker than the correlation found in Table III. Once again, we would point out the distinction between statistical significance and physical significance. For most practical purposes two particles in a cohort (even particles 8 and 9) move in a statistically independent fashion. Nevertheless, the data do seem to justify the tentative conclusion that particles can sometimes move in a weakly correlated fashion. These correlations could arise because of hydrodynamic interactions between the particles (2), because the correction for cell motion has not been completely effective, or because particles sometimes can become immobilized simultaneously.

TABLE IV

Kendall's Statistic for Correlation between Paired Observations*[a,b]

k_1	k_2	$\Delta Y_{i,k_1}$ $\Delta Y_{i,k_2}$	$\Delta Y_{i,k_1}$ $\Delta Y_{i+1,k_2}$	$\Delta Y_{i,k_1}$‡ $\Delta Y_{i,k_2}$	0.95 Critical level
1	2	−0.24	−0.17	−0.24	±0.35
1	3	−0.04	+0.22	−0.04	±0.35
1	4	−0.22	+0.20	−0.04	±0.35
2	3	−0.04	+0.28	−0.04	±0.35
2	4	+0.34	+0.02	+0.34	±0.35
3	4	−0.18	+0.27	−0.12	±0.35
5	6	+0.13	−0.05	+0.13	±0.30
5	7	+0.09	+0.13	+0.09	±0.30
6	7	+0.06	+0.07	+0.06	±0.30
8	9	+0.19	−0.06	+0.12	±0.15

* τ_k defined by Eq. 8 *a*.

‡ Restricted to these *i* for which $|\Delta Y_{i,k_1}| + |\Delta Y_{i,k_2}| > 0.05$ μm.

The conclusion that the particles of a cohort move in a uncorrelated (or at least quasi-uncorrelated) fashion implies that step-size distribution of the relative motion of two particles will have pooled variance $\sigma^2_{p,jk} = \sigma^2_{p,j} + \sigma^2_{p,k}$. This relationship was checked and found to hold to within experimental error for the 10 particle pairs of Table IV (data not shown).

DISCUSSION

In the Appendix, we present physical arguments that show that the most plausible explanation for our observation with $\sigma_x^2 \approx \sigma_y^2$ (see Fig. 4) is that the dominant contribution to the variable component to the force on a particle comes from thermal agitation. If we accept this conclusion, then the diffusion coefficient of a particle can be calculated according to the Einstein relation

$$D = \frac{k_b T}{f} = \frac{\sigma^2}{2\Delta t}. \tag{10}$$

In this equation, f is the fractional coefficient for lateral motion of the particle in the cell membrane, $k_b T$ is Boltzmann's constant × the absolute temperature, and σ^2 is the variance of the step size in a time interval Δt.

The Appendix also shows (Eq. A2) that the average velocity of a particle is given by

$$v = F_c/f = \mu_x/\Delta t \tag{11}$$

where F_c is the average force exerted by the cell on the particle. Note that because $k_b T \approx 4.1 \times 10^{-14}$ erg is a known constant, f can be obtained independently from the diffusion constant by means of Eq. 10. This means that Eq. 11 can be used to calculate F_c. Table V gives a summary of the best estimates of D, v, f, and F_c, for the various particles we have studied.

The use of the value of the pooled variance to approximate the value of σ^2 in Eq. 10 involves the implicit assumption that there is negligible experimental error in the measurement of particle position. In general, the pooled variance will be given by the sum of the variance in positional change resulting from true diffusion and the apparent variance resulting from experimental error, σ^2_{er}. As discussed previously (see Materials and Methods), we estimate a conservative upper limit for the value of σ^2_{er} of 0.02 μm^2. This would represent a large correction to the value of $\sigma^2_{p,k}$ for particle 9 and a 50% correction for particles 2 and 7 (see Table II). The exact magnitude of σ^2_{er} is difficult to determine. Furthermore, even if σ^2_{er} were as large as the upper limit of 0.02 $\mu_m{}^2$, it would not substantively affect our conclusions. Therefore, we have neglected the value of σ^2_{er} in calculating the numbers presented in Table V.

It is interesting to examine the numbers in Table V for consistency with other experimental systems and with various theoretical considerations.

The frictional coefficients of the particles in Table V range between 4×10^{-4} and 4×10^{-3} gm/s. From the data in Table I, we see that the effective radius of the particles is always between 0.5 and 1 μm. Application of Stokes' law shows that particles of this size have frictional coefficients in water of between 10^{-5} and 2×10^{-5} gm/s. As we would expect, this indicates that the fractional coefficient of the particles is dominated by the effects of contact with the membrane; the fact that the particles are also in contact with water is a minor perturbation.

TABLE V

*Estimated Parameters of Particle Motion**

Index k	v	D	f	F_c
	$\times 10^5$ cm/s	$\times 10^{10}$ cm^2/s	$\times 10^4$ gm/s	$\times 10^9$ dyn
1	0.19 ± 0.20	1.19 ± 0.53	3.45 ± 1.6	0.655 ± 1.0
2	0.32 ± 0.10	0.20 ± 0.09	20.50 ± 9.4	6.560 ± 5.1
3	0.30 ± 0.15	0.37 ± 0.16	11.08 ± 4.9	3.324 ± 2.6
4	0.29 ± 0.10	0.34 ± 0.15	12.00 ± 5.4	3.497 ± 2.7
5	0.57 ± 0.35	2.96 ± 1.16	1.39 ± 0.5	0.792 ± 0.8
6	0.49 ± 0.10	0.27 ± 0.11	15.19 ± 5.9	7.443 ± 4.4
7	0.46 ± 0.08	0.19 ± 0.08	21.58 ± 8.4	9.927 ± 5.6
8	0.08 ± 0.06	0.51 ± 0.11	8.04 ± 1.8	0.643 ± 0.6
9	0.08 ± 0.04	0.13 ± 0.03	31.54 ± 7.3	2.523 ± 1.9
10	0.12 ± 0.07	0.31 ± 0.09	13.23 ± 3.7	1.587 ± 1.4

* Errors indicate 95% confidence limits.

Diffusion constants of macromolecules embedded in the cell membrane have been reported in the general range of 10^{-11}–10^{-9} cm^2/s (5, 10). The diffusion constants we obtain for the particles in Table V are in the range of 10^{-11}–10^{-10} cm^2/s. It is noteworthy that these values are of comparable magnitude. The data seem to indicate that the large size difference between typical macromolecules and our particles does not cause a proportional difference in the diffusion constant.

Several hydrodynamic calculations of the frictional coefficient and the diffusion coefficient of particles or macromolecules embedded in cell membranes have been carried out (17, 20). These calculations predict diffusion coefficients that are 10–100 times larger than most experimentally reported values of diffusion constants for macromolecules (10, 20). We find a similar discrepancy between these theories and our values for the diffusion constants of particles. It is interesting that in accord with our results the hydrodynamic calculations predict a very small effect of size on the diffusion constant.

Finally, we turn to the value of the constant component of the force on a particle. From Table V, this force is $\leq 10^{-8}$ dyn. Because 1 μm is a typical dimension of a particle, this force can be interpreted as 10^{-8} dyn/μm of the leading edge of a particle or $\sim 10^{-8}$ dyn/μm^2 of the contact area of the particle and the cell. These are very small forces when compared with other forces exerted by or on cells. For example, the shear force exerted by the advancing margin of a CHF cell as it moves over a surface has been reported to be $\geq 10^{-3}$ dyn/μm (13). F_c is also small compared with the force required to rupture a typical noncovalent chemical bond, $\sim 10^{-5}$ dyn (3), or the elastic modulus for stretching of an erythrocyte membrane, $\sim 10^{-4}$ dyn/μm^2 (14).

We can understand the physical reason for the extremely small relative values of F_c, from the fact that when a cell pulls on a particle the particle continuously yields by moving in the direction of the force. This yielding will prevent the force-generating mechanism from operating at maximum efficiency. If both the cell and the particle were inhibited from yielding, the isometric tension developed between the two might become very much larger than the forces we observe. A separate consideration is that the ability of cells to grip the particles by forming bonds may be less than in the case of firmly attached substrates since, after the formation of the first few bonds, the particle will be moving and hence be transported out of the part of the leading edge where new bonds can be formed.

Since k_bT is a constant for all particles, Eq. 10 implies that the only way to explain the 10-fold variation in $\sigma^2_{p,k}$ for different particles in the same cohort is in terms of differences in the fractional coefficients of the particles. From Table I, we see that differences in particle size or in the material of the particles cannot explain this variation. In our view, the only remaining alternative is to say that the frictional coefficient is determined in large part by the way in which a particular particle is attached to the cell. We find it useful to think of the particles physically as being held to the cell by adhesive bonds that are formed when the particle is first picked up by the cell. As a particle undergoes lateral movement in the cell membrane these bonds must move with the particle; the bonds thus transmit a viscous drag force to the particle as they rub against membrane or cytoplasmic structures. The frictional coefficient of this drag force should depend strongly on the number of adhesive bonds. This dependence could explain the large variation in the diffusion constant of different particles. On the other hand, the fact that the diffusion constant for a given particle remains constant during the course of its motion indicates that, once the bonds are established to a particle, they remain substantially fixed in number.

If we conditionally accept the evidence that the frictional coefficient of the particles within a cohort varies by a factor of 10, how can we explain the empirical observation that there is no detectable difference in the average velocity of the particles? From Eq. 11, it is clear that the average velocity should vary inversely with the frictional coefficient. Thus, to explain the constancy of the average velocity we are led to conclude that the average imposed force on a particle depends on the number of bonds in such a way as to exactly cancel the effect of f on Eq. 14.

A number of simple physical models could produce an imposed force proportional to the number of bonds. One such model is the "membrane flow" hypothesis proposed by Abercrombie et al. (1) on the basis of qualitative observations of the pattern of particle motion.

In recent years a number of studies that tend to contradict the original statement of the membrane flow hypothesis have been carried out (see, for example, Vasiliev et al. [19], Middleton [16], and Dembo et al. [7]). Nevertheless, it is possible to accommodate these objections within the basic spirit of Abercrombie's idea if we introduce the generalization that the flow driving particle motion can occur in the submembrane material rather than in the material of the membrane itself. This generalization involves the additional complication of requiring a mechanism for physically coupling the particle and the submembrane flow through the stationary material of the membrane. In addition, conservation of mass requires that the submembrane flow toward the rear of the cell be counterbalanced by a central flow toward the front of the cell (see Fig. 5 *a*).

Another simple model with a number of positive and negative features is the proposal that the adhesive bonds holding the particle to the cell are coupled to cortical contractile proteins in such a way that cycles of contraction, detachment, relaxation, and reattachment of the proteins cause each bond to experience independent propulsive forces. One can think of this mechanism as similar to propulsion by the beating of numerous cortical "cilia" that brush against the inside of the cell membrane and push the particles along. It must be assumed that the forces produced by the "cilia" somehow add up to produce a net force that on average is proportional to the number of bonds (see Fig. 5 *b*).

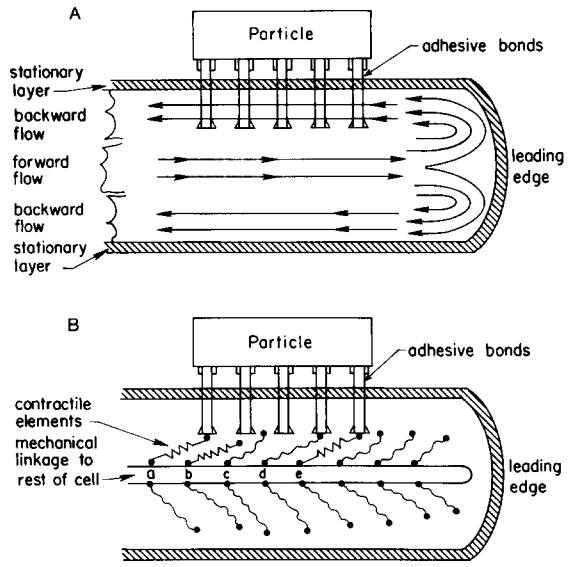

FIGURE 5 Two models of the mechanism of particle motion: (*A*) the cortical flow model, (*B*) the cortical "cilia" model. In *A*, the force on the particle is produced by submembrane fluid current in the lamelloplasm. In *b*, the force is produced by cycles of (*a*) contraction, (*b*) detachment, (*c*) relaxation, (*d*) attachment, and (*e*) recontraction of proteins in the lamelloplasm.

This model is unfortunately vague on many details. An additional difficulty with this model is that we would expect to detect differences in the random motion of the particles because of random variations in the activities of the cortical "cilia." Since we do not find this kind of variation (see Results), we are forced to add the assumption that the "cilia" beat in a very constant way so that variations in the force they produce are negligible compared with thermal fluctuations. Although it is possible that this is in fact the case, the hypothesis that the particles are pushed by flow of the membrane or of some submembrane material gives a more straightforward account of our observations.

A critical test to differentiate these two theories could be made if a larger number of particles were observed for extended periods or for shorter periods at small time intervals. Under these circumstances the error in determining σ_x^2 and σ_y^2 could be reduced and a small difference between σ_x^2 and σ_y^2 attributable to the action of the contractile elements could be detected. Failure to observe consistent differences between σ_x^2 and σ_y^2 under these conditions would further support the hypothesis of membrane or submembrane flow.

As a final model of particle motion, consider the hypothesis that each particle is attached to its own strand of cytoplasmic actomyosin. This strand must be anchored at one end near the center of the cell so that as it slowly contracts the particle is pulled centripetally. Allowing for elasticity of the actomyosin strand, thermal agitation could produce a random component of the particle motion. It is easy to see that according to this model a particle which lagged behind because of thermal agitation would be pulled up short, whereas one that was pushed ahead would feel a weakened rearward pull. This kind of effect would produce a strong correlation between the step sizes during successive time intervals; small steps would tend to be followed by large steps, and vice versa. Since such behavior is definitely not observed (see Table III), the contracting filament model can be rejected. The essential reason for the failure of this model is that it does not allow for a fluid coupling between the particle and the cellular propulsion mechanism. Both Abercrombie's hypothesis and the cortical flow hypothesis incorporate the concept of fluid coupling.

None of the models we have discussed can account for the unusual temporary immobilization exhibited by particles 8 and 9 (see Results). This phenomenon is reminiscent of the fraction of immobile cell surface receptors commonly observed with the fluorescence photobleaching recovery technique (10). A number of possibilities exist to explain temporary immobilization; among these are local spontaneous transitions to a liquid crystalline state of the liquid-protein lattice and anchorage to the cytoskeleton. Immobilization and the related phenomenon of correlations between adjacent particles deserve to be analyzed in a more detailed way than has been possible in the present study.

There are a number of possible extensions of our results to the study of larger issues in cell mobility. For example, in the area of chemotaxis it will be interesting to see if exposure to chemotactic gradients produces differential effects on the motion of particles on the near vs. far side of the cell. It will also be of interest to see if chemotactic substances affect the velocity (i.e., force per adhesive bond) as opposed to the diffusion constant (i.e., number of adhesive bonds) of particles being transported by cells and the time-course with which these possible effects are expressed. Another interesting avenue of research will be the effect of coating particles with various quantities of agents such as fibronectin, which are reputed to mediate adhesion. Our model of particle transport would predict an effect of fibronectin density on the diffusion constant of particles but not on the average velocity of transport.

APPENDIX

Consider a particle with very small mass, m, moving in a two-dimensional viscous fluid. We assume that the particle is under the influence of the usual rapidly varying thermal forces, $\vec{R}(t) = [R_x(t), R_y(t)]$, as well as an imposed force of unknown origin. The magnitude of the imposed force can always be written as the sum of a constant term F_c and a variable term $\nu(t)$. In addition, we can choose F_c such that the ensemble average of $\nu(t) = 0$. Newton's law for the particle we have described takes the form of the Langevin equations

$$m\frac{d^2}{dt^2}X = -f\frac{d}{dt}X + [F_c + \nu(t)]\cos[\theta(t)] + R_x(t)$$

and

$$m\frac{d^2}{dt^2}Y = -f\frac{d}{dt}Y + [F_c + \nu(t)]\sin[\theta(t)] + R_y(t), \quad \text{(A.1)}$$

where f denotes the frictional coefficient of the particle and $\theta(t)$ gives the angular direction of the imposed force.

The imposed force on the particle is clearly attributable to some mechanism contained in the leading lamella. Thus, the fact that the leading lamella has a highly polarized and slowly changing morphology suggests that the imposed force should have a fairly constant direction. This is also indicated by the observations that the average direction of different particles at different locations on the membrane is the same, and that the direction of motion of individual particles remains constant in time. Consequently, we will restrict our attention to those cases where $\theta(t)$ varies within a moderate range ($\pm 45°$) around $\theta = 0$. For this special case we can assume that $\cos[\theta(t)] \approx 1$ and $\sin[\theta(t)] \approx \theta(t)$.

Carrying through a standard argument completely analogous to the derivation of the step-size distribution for a free Brownian particle (18), it can be shown that for macroscopic time intervals (Δt), $\Delta X = X(\Delta t) - X(0)$ and $\Delta Y = Y(\Delta t) - Y(0)$ will be independent Gaussian random variables with means

$$\mu_x = \frac{1}{f} F_c \Delta t \tag{A.2}$$

and

$$\mu_y = 0. \tag{A.3}$$

The variances of ΔX and ΔY are

$$\sigma_x^2 = \frac{\Delta t}{f^2} \overline{\nu^2} \tau_\nu + \frac{2k_bT}{f} \Delta t \tag{A.4}$$

and

$$\sigma_y^2 = \frac{\Delta t \overline{\theta^2}(t)}{f^2} [F_c{}^2 \tau_\theta + \overline{\nu^2} \tau_{\theta,\nu}] + \frac{2k_bT}{f} \Delta t \tag{A.5}$$

In these equations, k_bT is Boltzmann's constant times the absolute temperature, τ_ν and τ_θ represent the characteristic "correlation times" of the random fluctuation in $\nu(t)$ and $\theta(t)$, respectively, and the bar symbol (—) denotes the ensemble average of a quantity. $\tau_{\nu,\theta}$ represents the correlation time of the product $\nu(t)\theta(t)$; it will be less than the smaller of τ_θ and τ_ν but will approach $\min[\tau_\theta, \tau_\nu)$ if one of these quantities is very much less than the other.

If k_bT/f is negligible compared with the other terms on the right-hand side of Eqs. A.4 and A.5, then it is possible by a fortuitous choice of the parameters to satisfy the condition that $\sigma_x^2 \approx \sigma_y^2$. However, this choice of parameters is completely ad hoc, has no physical significance, and occurs with probability zero. Therefore, in general the observation that $\sigma_x^2 \approx \sigma_y^2$ (see Fig. 4) will be violated unless k_bT/f is the dominant term on the right side of Eqs. A.4 and A.5. This simply means that, physically, the fluctuations in position attributable to thermal agitation dominate the fluctuations produced by variations in the imposed force.

The authors wish to thank George Bell and William W. Wood for helpful discussions during the preparation of this manuscript.

Work by M. Dembo was done under the auspices of the U. S. Department of Energy. A. K. Harris was supported by National Institutes of Health grant GM24251 and by a fellowship from the Damon Runyon–Walter Winchell Fund for Cancer Research.

Received for publication 28 April 1981, and in revised form 20 July 1981.

REFERENCES

1. Abercrombie, M., J. E. M. Heaysman, and S. M. Pegram. 1970. The locomotion of fibroblasts in culture. III. Movements of particles on the dorsal surface of the leading lamella. *Exp. Cell Res.* 62:389–398.
2. Aguirre, J. L., and T. J. Murphy. 1973. Brownian motion of *n* interacting particles. II. Hydrodynamical evaluation of the diffusion tensor matrix. *J. Chem. Phys.* 59:1833–1840.
3. Bell, G. I. 1978. Models for the specific adhesion of cells to cells. *Science (Wash. D. C.).* 200:618–627.
4. Bray, D. 1970. Surface movements during growth of single explanted neurons. *Proc. Natl. Acad. Sci. U. S. A.* 65:905–910.
5. Cherry, R. J. 1979. Rotational and lateral diffusion of membrane proteins. *Biochim. Biophys. Acta.* 559:289–327.
6. Conover, W. J. 1971. Practical Nonparametric Statistics. John Wiley & Sons, Inc., New York.
7. Dembo, M., L. Tuckerman, and W. Goad. 1981. Motion of polymorphonuclear leukocytes: theory of receptor redistribution and the frictional force on a moving cell. *Cell Motility* 1: 205–235.
8. DiPasquale, A. 1975. Locomotory activity of epithelial cells in culture. *Exp. Cell Res.* 94: 191–215.
9. DiPasquale, A., and P. B. Bell. 1974. The upper cell surface: its inability to support active cell movement in culture. *J. Cell Biol.* 62:198–214.
10. Flanagan, M. T. 1980. More light on membrane protein mobility. *Nature (Lond.).* 284: 126–126.
11. Harris, A. K. 1973. Cell surface movements related to locomotion. *In* Locomotion of Tissue Cells. *Ciba Found. Symp.* 14(d):3–20.
12. Harris, A. K., and G. Dunn. 1972. Centripetal transport of attached particles on both surfaces of moving fibroblasts. *Exp. Cell Res.* 73:519–523.
13. Harris, A. K., P. Wild, and D. Stopak. 1980. Silicone rubber substrata: a new wrinkle in the study of cell locomotion. *Science (Wash. D. C.).* 208:177–179.
14. Hochmuth, R., M. N. Mohandas, and P. L. Blackshear. 1973. Measurement of the elastic modulus for red cell membrane using a fluid mechanical technique. *Biophys. J.* 13:747–762.
15. Ingram, Y. M. 1969. A side view of moving fibroblasts. *Nature (Lond).* 222:641–644.
16. Middleton, C. A. 1979. Cell surface labeling reveals no evidence for membrane assembly and dissembly during fibroblast locomotion. *Nature (Lond.).* 203–205.
17. Saffman, P. G., and M. Delbruck. 1975. Brownian motion in biological membranes. *Proc. Natl. Acad. Sci. U. S. A.* 72:3111–3113.
18. Uhlenbeck, G. E., and L. S. Ornstein. 1930. On the theory of the Brownian motion. *Phys. Rev.* 36:823–841.
19. Vasiliev, J. M., I. M. Gelfand, L. V. Domivina, N. A. Dorfman, and O. Y. Pletyushkina. 1976. The active cell edge and movements of concanavalin A receptors of the surface of epithelial and fibroblastic cells. *Proc. Natl. Acad. Sci. U. S. A.* 73:4085–4089.
20. Wiegel, F. W. 1980. Fluid flow through porous macromolecular systems. *Lect. Notes Phys.* 121:54–76.